Electronic Supplementary Material (ESI) for Journal of Materials Chemistry A.

Supporting Information

Electronic doping-enabled transition from n- to p-type conductivity over Au@CdS core-shell nanocrystals toward unassisted photoelectrochemical water splitting

Rongrong Pan, Jia Liu,* Yuemei Li, Xinyuan Li, Erhuan Zhang, Qiumei Di, Mengyao Su and Jiatao Zhang*

Beijing Key Laboratory of Construction Tailorable Advanced Functional Materials and Green Applications, School of Materials Science and Engineering, Beijing Institute of Technology, Beijing 100081, China

Supplementary Data

Table S1. The elemental compositions of the Au@CdS core-shell HNCs derived from Au@Ag_2S core-shell HNCs by cation exchange. The addition amounts of $Cd(NO_3)_2 \cdot 4H_2O$ and TBP during the Cd^{2+}-for-Ag^+ cation exchange process were varied for Au@CdS-1 and Au@CdS-2 (Specifically, 0.25 g of $Cd(NO_3)_2 \cdot 4H_2O$ and 100 μL of TBP for Au@CdS-1; 0.03 g of $Cd(NO_3)_2 \cdot 4H_2O$ and 50 μL of TBP for Au@CdS-2). Determined by XPS analysis.

Sample	Atomic concentration (S2p, %)	Atomic concentration (Ag3d, %)	Atomic concentration (Cd3d, %)
Au@CdS-1	49.2	1.9	48.9
Au@CdS-2	47.7	8.7	43.6

Table S2. The elemental compositions of the Cu-doped Au@CdS core-shell HNCs determined by XPS analysis.

Sample	Atomic concentration (S2p, %)	Atomic concentration (Cu2p, %)	Atomic concentration (Cd3d, %)
Cu(6.3)-Au@CdS	54.6	6.3	39.1
Cu(14.7)-Au@CdS	47.5	14.7	37.8
Cu(16.6)-Au@CdS	45.5	16.6	37.9
Cu(18.9)-Au@CdS	41.2	18.9	39.9

Table S3. Summarization of the conductivity type, carrier density, and flat band potential of undoped and Cu-doped Au@CdS core-shell HNCs with different dopant concentration. Determined by the Mott-Schottky equation.

Sample	Type	N (cm^{-3})	Flat band potential (V vs RHE)
Au@CdS	n	1.7×10^{19}	-0.08
Cu(6.3)-Au@CdS	n	9.7×10^{18}	0.27
Cu(14.7)-Au@CdS	p	1.7×10^{19}	1.87
Cu(16.6)-Au@CdS	p	2.1×10^{19}	1.91
Cu(18.9)- Au@CdS	p	8.8×10^{19}	1.99

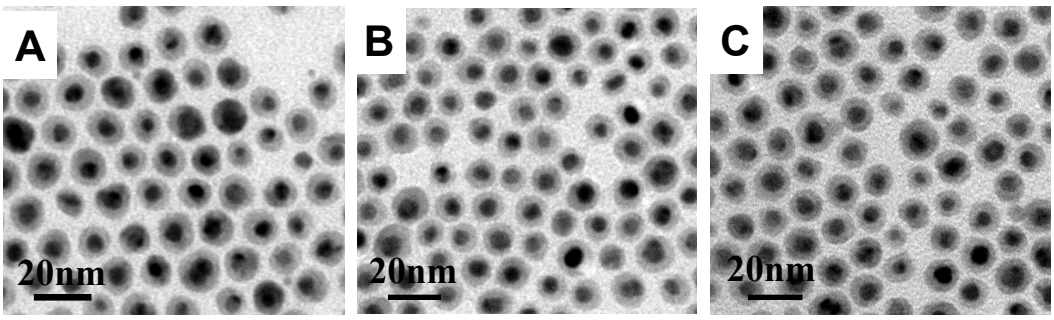

Fig. S1. TEM images of pristine Au@CdS core-shell HNCs (A), Au@Cu_2S core-shell HNCs (B) and Cu-doped Au@CdS core-shell HNCs (C).

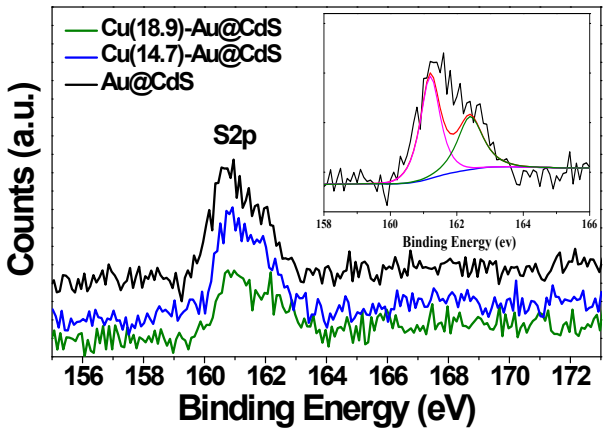

Fig. S2. XPS spectra of S2p for the undoped and Cu-doped Au@CdS core-shell HNCs.

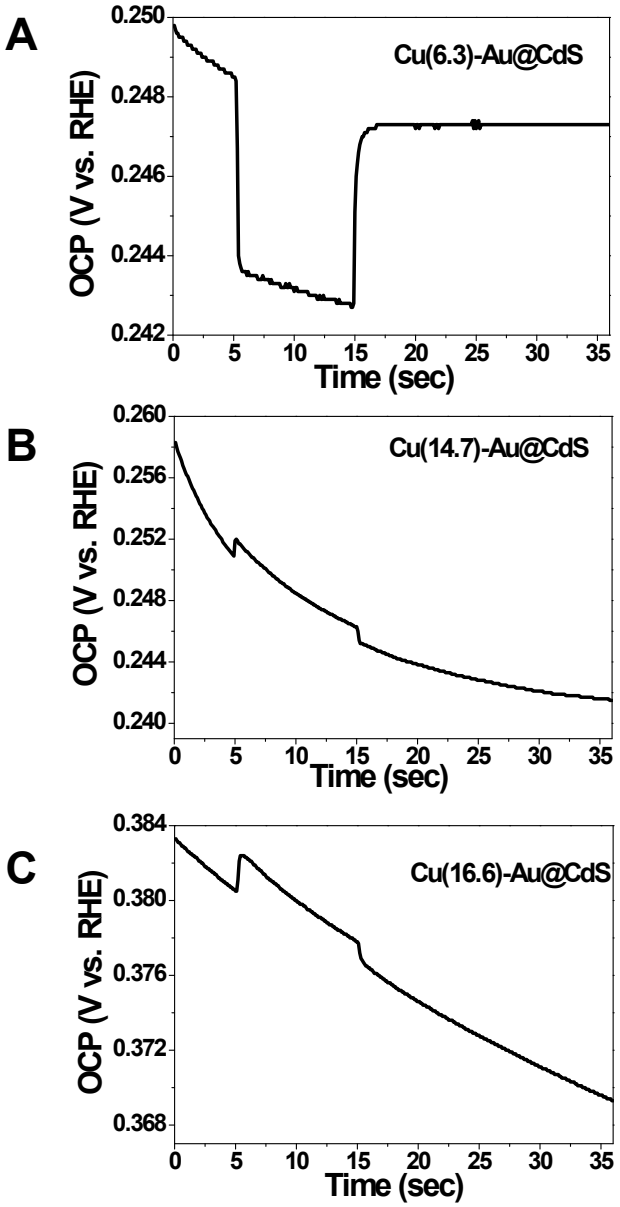

Fig. S3. OCP responses of the Cu-doped Au@CdS core-shell HNCs with different dopant concentrations under illumination and in the dark. (A) Cu(6.3)-Au@CdS, (B) Cu(14.7)-Au@CdS, and (C) Cu(16.6)-Au@CdS.

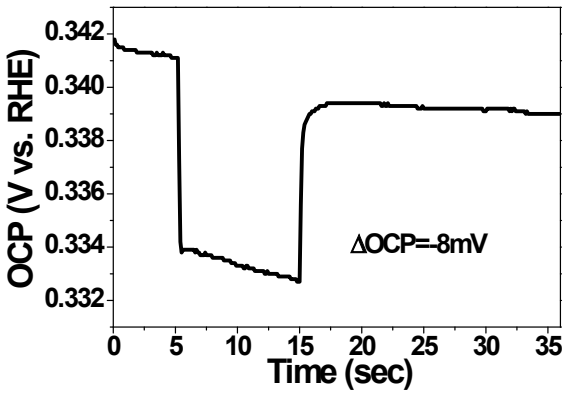

Fig. S4. OCP response of Cu-doped Au@CdS with notable Ag impurities in the shell matrix. Specifically, here Au@CdS-2 HNCs were adopted as the starting materials, which were prepared from Au@Ag_2S core-shell HNCs by incomplete cation exchange involving the usage of 0.03 g of $Cd(NO_3)_2 \cdot 4H_2O$ and 50 μL of TBP (Table S1). Although the reaction conditions for subsequent synthesis were the same as those for Cu(18.9)-Au@CdS core-shell HNCs, the ΔOCP value of this sample was still highly negative indicating the n-type conductivity. This was probably ascribed to the existence of the Ag impurities in the shell matrix, suggesting that the full removal of the Ag ions from the shell is a prerequisite for switching the conductivity type from n to p for the final products.

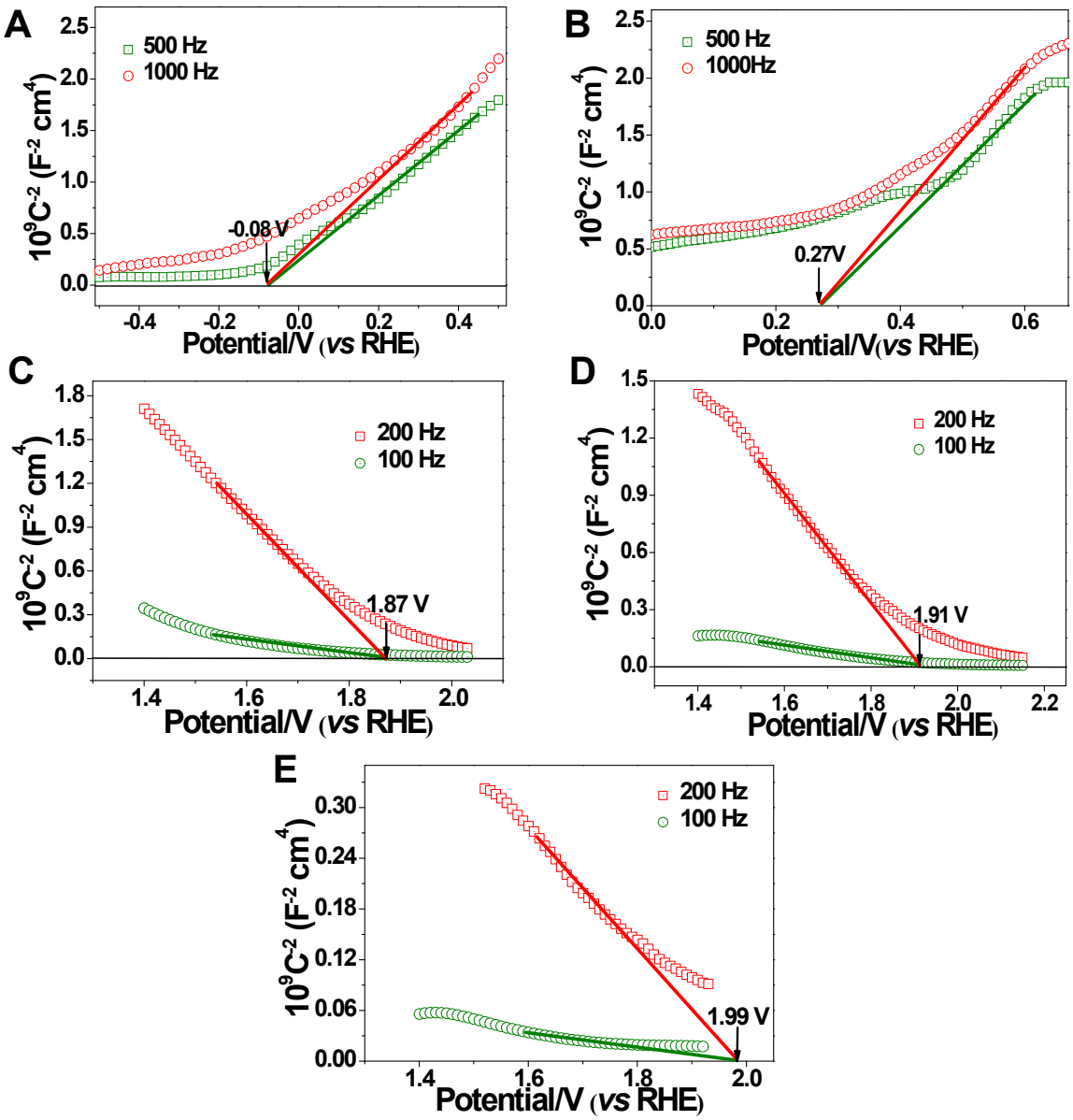

Fig. S5. Results of Mott-Schottky measurements for (A) undoped Au@CdS, (B) Cu(6.3)-Au@CdS, (C) Cu(14.7)-Au@CdS, (D) Cu(16.6)-Au@CdS and (E) Cu(18.9)-Au@CdS core-shell HNCs at different modulation frequencies.

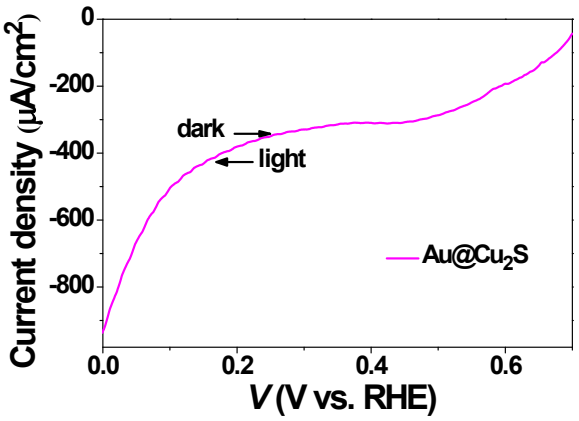

Fig. S6. Photocurrent density-potential curve for $Au@Cu_2S$ core-shell HNCs under simulated sunlight illumination (AM 1.5G, 100 mW cm^{-2}) using a three-electrode configuration.

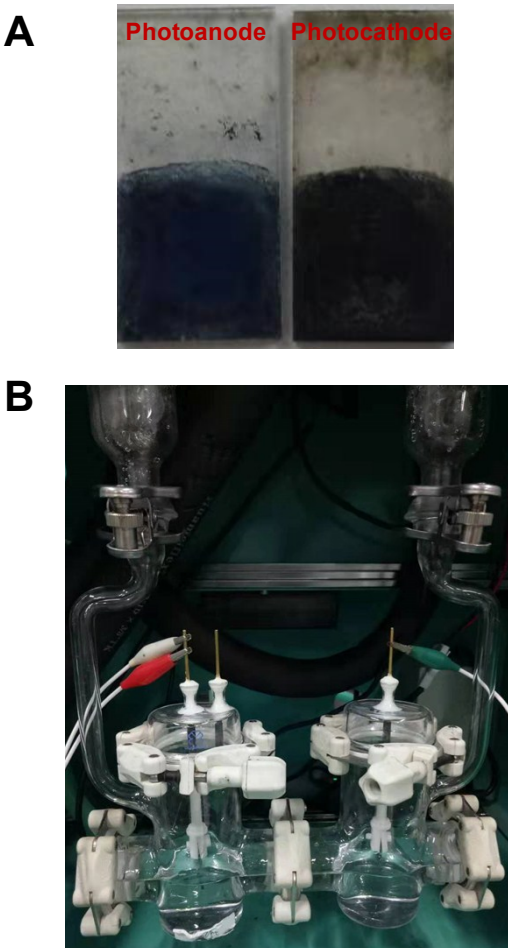

Fig. S7. Photographs of the IrO_x/Au@CdS photoanode and NiS/Cu(14.7)-Au@CdS photocathode (A) and the constructed tandem PEC cell (B).

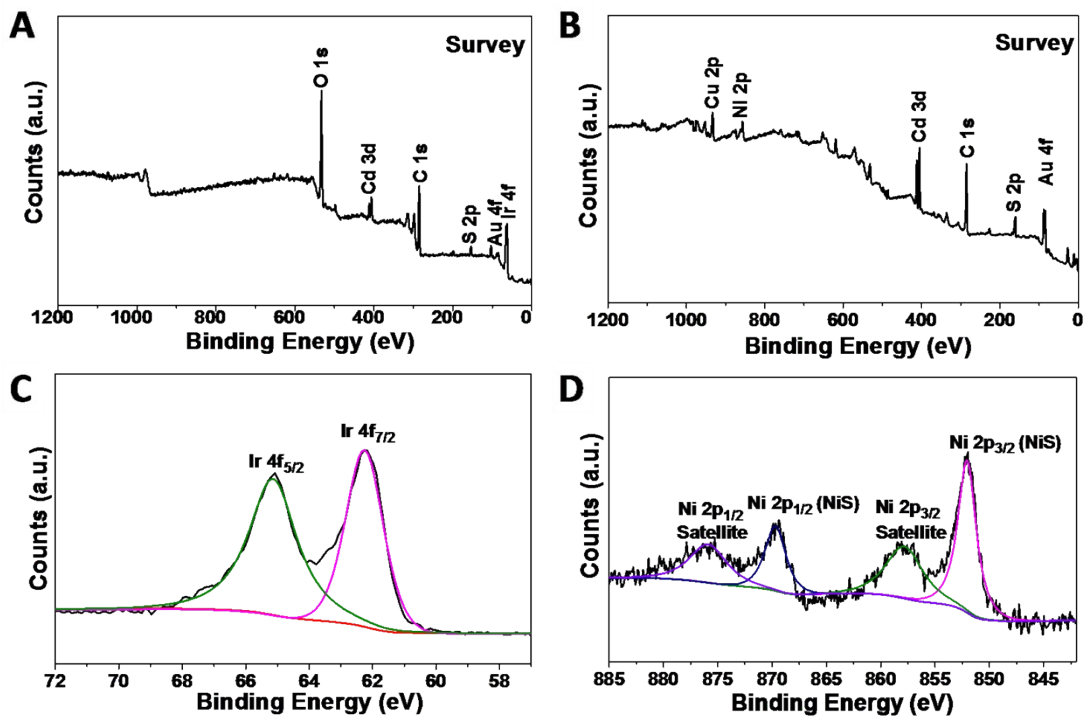

Fig. S8. XPS spectra for IrO_x/Au@CdS photoanode (A,C) and NiS/Cu(14.7)-Au@CdS photocathode (B,D).

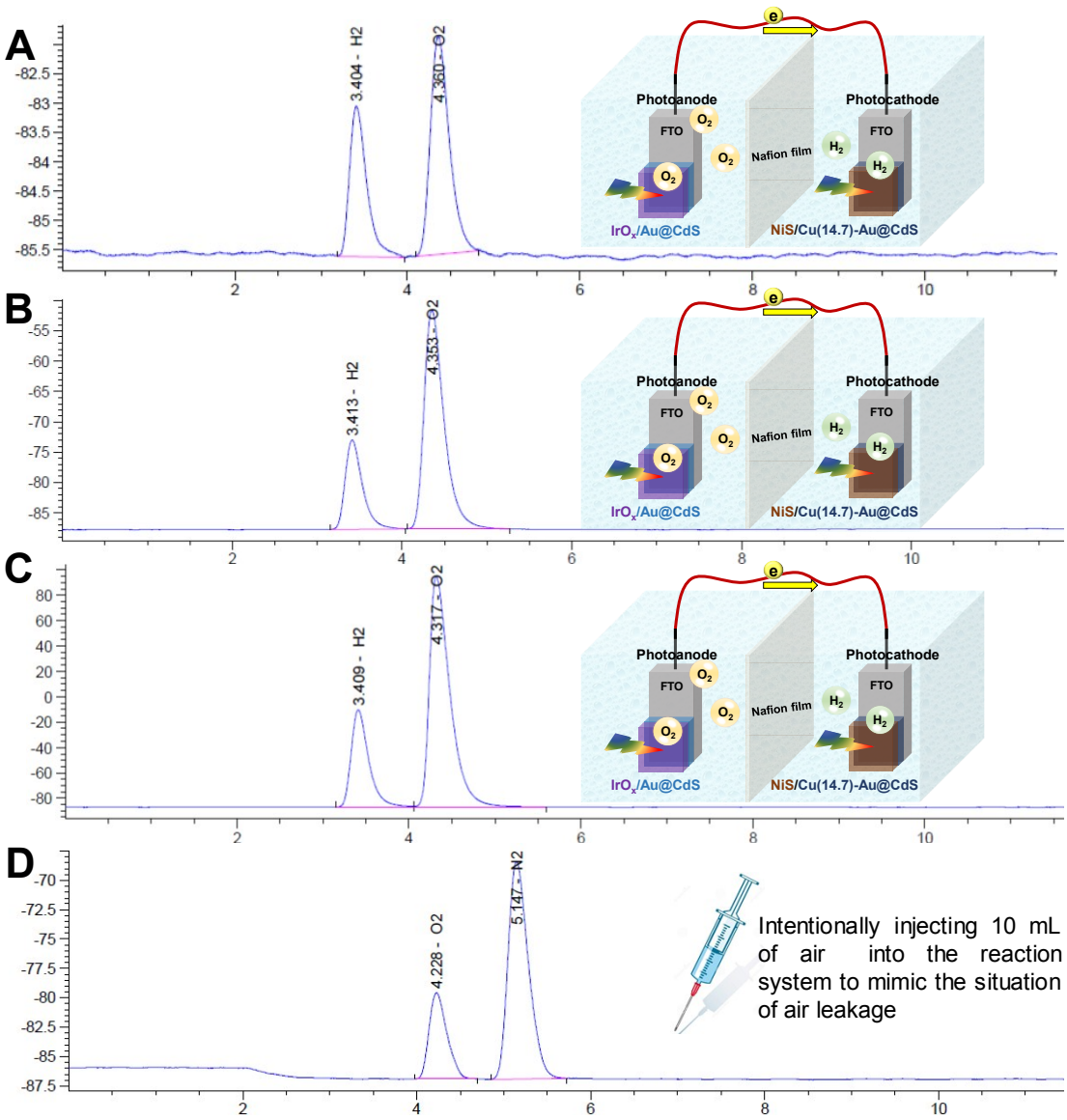

Fig. S9. (A-C) The original gas chromatographic data for the evolution of O_2 and H_2 over time generated by the constructed tandem PEC cell, where the peaks of H_2 and O_2 appeared at about 3 minutes and 4 minutes, respectively. (D) The data was measured by gas chromatograph after 10 mL of air was intentionally injected into the reaction system, where the peaks of O_2 and N_2 appeared at about 4 minutes and 5 minutes, respectively.

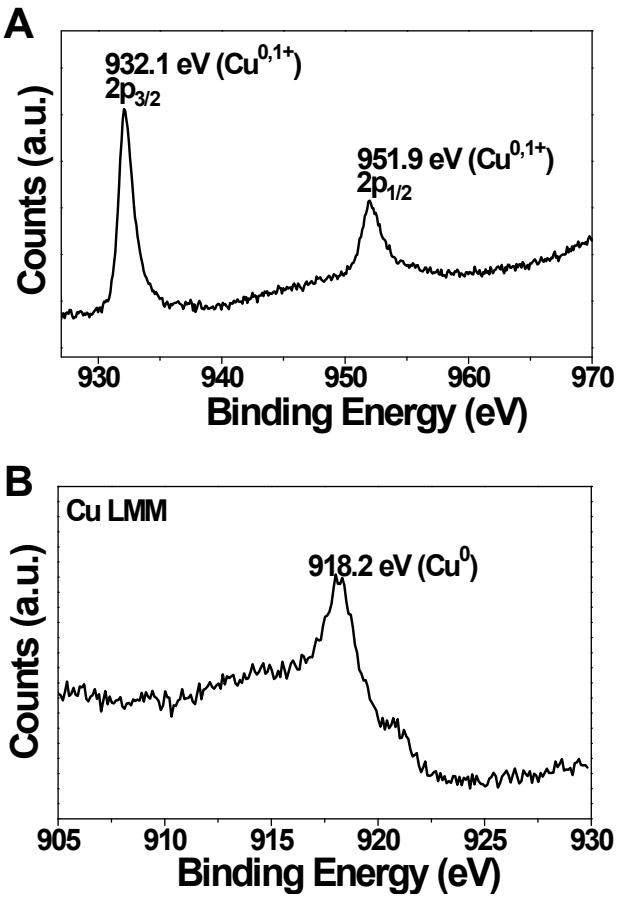

Fig. S10. XPS spectra of (A) Cu 2p and (B) Auger spectra of Cu LMM for the photocathode material (Cu(14.7)-Au@CdS HNCs decorated with NiS) of the constructed tandem PEC cell after PEC water splitting reaction. The results demonstrated that the vast majority of Cu in photocathode showed 0 valence,[1,2] suggesting that a considerable amount of accumulated electrons at the photocathode surface were consumed by the Cu dopant instead of the protons in solution to produce hydrogen.

References

1 X. Y. Zhu, H. P. Rong, X. B. Zhang, Q. M. Di, H. S. Shang, B. Bai, J. J. Liu, J. Liu, M. Xu, W. X. Chen and J. T. Zhang, *Nano res.*, 2019.

2 X. F. Dai, W. Xu, T. Zhang, H. B. Shi and T. Wang, *Chem. Eng. J.,* 2019, **364**, 310-319.